Nano Research
DOI 10.1007/s12274-015-0712-3
Research Article
ISSN 1998-0124
CN 11-5974/O4

Gold nanoparticles/ZnO nanorods hybrids for enhanced reactive oxygen species generation and photodynamic therapy

Zhuo Kang[1], Xiaoqin Yan[1], Lanqing Zhao[2], Qingliang Liao[1], Yi Liu[1], Zheng Zhang[1], Kun Zhao[1], Hongwu Du[2], Xiaohui Zhang[1], Pei Lin[1], Zhiming Bai[1], Yue Zhang[1,3] (✉)

Nano Res., **Just Accepted Manuscript** • DOI 10.1007/s12274-015-0712-3
http://www.thenanoresearch.com on January 6, 2015

© Tsinghua University Press 2015

Just Accepted

This is a "Just Accepted" manuscript, which has been examined by the peer-review process and has been accepted for publication. A "Just Accepted" manuscript is published online shortly after its acceptance, which is prior to technical editing and formatting and author proofing. Tsinghua University Press (TUP) provides "Just Accepted" as an optional and free service which allows authors to make their results available to the research community as soon as possible after acceptance. After a manuscript has been technically edited and formatted, it will be removed from the "Just Accepted" Web site and published as an ASAP article. Please note that technical editing may introduce minor changes to the manuscript text and/or graphics which may affect the content, and all legal disclaimers that apply to the journal pertain. In no event shall TUP be held responsible for errors or consequences arising from the use of any information contained in these "Just Accepted" manuscripts. To cite this manuscript please use its Digital Object Identifier (DOI®), which is identical for all formats of publication.

TSINGHUA UNIVERSITY PRESS Springer

Template for Preparation of Manuscripts for *Nano Research*

This template is to be used for preparing manuscripts for submission to *Nano Research*. Use of this template will save time in the review and production processes and will expedite publication. However, use of the template is not a requirement of submission. Do not modify the template in any way (delete spaces, modify font size/line height, etc.). If you need more detailed information about the preparation and submission of a manuscript to Nano Research, please see the latest version of the Instructions for Authors at http://www.thenanoresearch.com/.

TABLE OF CONTENTS (TOC)

Authors are required to submit a graphic entry for the Table of Contents (TOC) in conjunction with the manuscript title. This graphic should capture the readers' attention and give readers a visual impression of the essence of the paper. Labels, formulae, or numbers within the graphic must be legible at publication size. Tables or spectra are not acceptable. Color graphics are highly encouraged. The resolution of the figure should be at least 600 dpi. The size should be at least 50 mm × 80 mm with a rectangular shape (ideally, the ratio of height to width should be less than 1 and larger than 5/8). One to two sentences should be written below the figure to summarize the paper. To create the TOC, please insert your image in the template box below. Fonts, size, and spaces should not be changed.

Gold nanoparticles/ZnO nanorods hybrids for enhanced reactive oxygen species generation and photodynamic therapy

Zhuo Kang[1], Xiaoqin Yan[1], Lanqing Zhao[2], Qingliang Liao[1], Yi Liu[1], Zheng Zhang[1], Kun Zhao[1]，Hongwu Du[2], Xiaohui Zhang[1], Pei Lin[1], Zhiming Bai[1], Yue Zhang[1,3,*]

[1]State Key Laboratory for Advanced Metals and Materials, School of Materials Science and Engineering, University of Science and Technology Beijing, Beijing 100083, China
[2]Department of Biotechnology, School of Chemistry and Biology Engineering, University of Science and Technology Beijing, Beijing 100083, China
[3]Key Laboratory of New Energy Materials and Technologies, University of Science and Technology Beijing, Beijing 100083, China

Page Numbers. The font is ArialMT 16

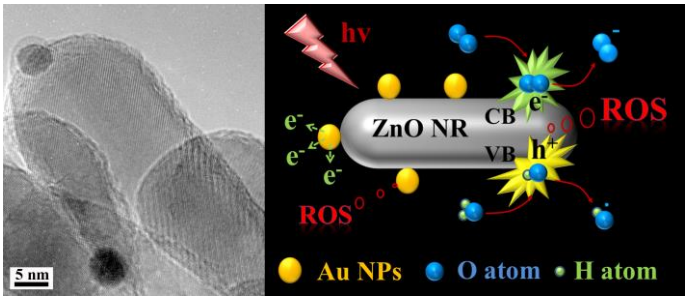

This work demonstrated the enhanced reactive oxygen species generation of Au nanoparticle /ZnO nanorod hybrids under UV illumination, and further confirmed the feasibility of adopting such hybrids for photodynamic therapy treatment.

Yue Zhang, nano.ustb.edu.cn/

Nano Res
DOI (automatically inserted by the publisher)
Research Article

Gold nanoparticles/ZnO nanorods hybrids for enhanced reactive oxygen species generation and photodynamic therapy

Zhuo Kang[1], Xiaoqin Yan[1], Lanqing Zhao[2], Qingliang Liao[1], Yi Liu[1], Zheng Zhang[1], Kun Zhao[1], Hongwu Du[2], Xiaohui Zhang[1], Pei Lin[1], Zhiming Bai[1], Yue Zhang[1,3] (✉)

[1] State Key Laboratory for Advanced Metals and Materials, School of Materials Science and Engineering, University of Science and Technology Beijing, Beijing 100083, China

[2] Department of Biotechnology, School of Chemistry and Biology Engineering, University of Science and Technology Beijing, Beijing 100083, China

[3]Key Laboratory of New Energy Materials and Technologies, University of Science and Technology Beijing, Beijing 100083, China

Received: day month year / Revised: day month year / Accepted: day month year (automatically inserted by the publisher)
© Tsinghua University Press and Springer-Verlag Berlin Heidelberg 2014

ABSTRACT

Gold nanoparticles (Au NPs)@ZnO nanorods (NRs) hybrids, with various molar ratios of ZnO:Au, were developed to enhance generation of reactive oxygen species (ROS) for further application in photodynamic therapy (PDT). By introducing the metal/semiconductor heterostructure interface between Au NPs and ZnO NRs, the electron transfer was modulated under UV irradiation, which dramatically suppressed the electron-hole recombination in ZnO, and simultaneously increased the amount of excited electrons with high energy at Au NPs' surface. Hence, the ROS yield of the nanohybrid was considerably improved compared with pristine Au NPs or pristine ZnO NRs, demonstrating the 1 + 1 > 2 effect. Moreover, such enhancement was strengthened along with the increase of Au proportion in the hybrid. It was exhibited that the Au@ZnO (ZnO:Au=20:1) acquired the highest ROS yield due to the largest interface area between Au and ZnO, which in turn led to the lowest cell viability for Hela and C2C12 cells during PDT. Besides, both ROS generation and cell destruction have positive correlation with nanohybrid dosage. The Au@ZnO hybrid (20:1,100 μg/ml) resulted in the Hela cell viability as low as 28% after UV exposure for 2 min, indicating a promising potential for therapeutic efficacy improvement in PDT.

KEYWORDS

gold nanoparticles; ZnO nanorods; reactive oxygen species; photodynamic therapy

1 Introduction

Photodynamic therapy (PDT) has been well developed in past decades as an alternative method to the traditional treatment in different oncologic field because it promises a better selectivity for tumor tissue that is accessible to light and low systemic toxicity compared to the chemotherapy and radiation therapy [1-3]. In the past decades, PDT has been applied for the treatment of early lung cancer

Address correspondence to yuezhang@ustb.edu.cn

[4], head and neck cancers [5], bladder cancer [6], and skin cancer [7]. PDT is based on the photochemical reactions of photosensitizing agent (PS) who is capable of generating cytotoxic reactive oxygen species (ROS) to kill tumor cell when exposed to light of appropriate wave-length [8-11]. ROS include free radicals such as superoxide anion (O_2^-), hydroxyl radical (·OH), as well as nonradical molecules like hydrogen peroxide (H_2O_2), singlet oxygen (O_2), which formed upon incomplete reduction of oxygen [12]. When the level of ROS exceeds the defense mechanisms, they can pose a threat to cells by causing peroxidation of lipids, oxidation of proteins, damage to nucleic acid, and ultimately lead to various diseases and cell apoptosis and necrosis [13]. Therefore, enhanced ROS generation is crucial for PDT of cancer.

Various PSs have been approved for clinical PDT, such as porphyrins like porfimer sodium and protoorphyrin Ⅸ, chlorins like verteporfin and temoporfin, as well as phthalocyanines like sulphonated aluminlum phthalocyanine mixture [14]. Recently, semiconductor nanomaterials are believed to have potentially promising future in PDT due to their unique phototoxic effect with the irradiation. Nano-scale ZnO, with direct wide band gap energy of 3.37ev at room temperature, can generate ROS in aqueous media under ultraviolet (UV) illumination. Since the UV light can be applied locally during PDT treatment, it is possible to reach an approach for conveying selective damage to targeted cancer cells, while sparing neighboring untargeted cells. It has been demonstrated that ZnO nanostructures were employed to efficiently kill cancer cells through the release of ROS [15-20]. And the antibacterial activity of ZnO nanoparticles originated from ROS induced membrane lipid peroxidation was verified [21]. On the other hand, Au nanostructures, such as nanoparticles (NPs) [22-27], nanorods [28-34], nanocages [35, 36], and nanoshells [37, 38], were developed as effective therapeutic tools in applications of photothermal therapy (PTT) [25, 28-35, 38] or PDT [22-24, 27, 28, 33-35] to induce cellular damage either via extensive temperature rise or considerable ROS generation. Specifically for Au NPs in PDT, ROS generation of Au NPs with diameters of 5-250 nm in water was investigated, indicating an inverse proportion of ROS quantity to the Au NPs' diameter, and thus suggests that larger surface area of Au NPS is more favorable for ROS yield [22]. In addition, the size-dependent enhancement of ROS formation enabled by protoporphyrin IX conjugated with Au NPs in human breast cancer cells (MDA-MB-231) was also confirmed [23]. With the aid of antibody-coated Au NPs, the selective damage was conveyed to targeted cancer cells based on ROS accumulation within cells after femtosecond pulse irradiation [24]. More recently, Au NPs were deposited on ZnO NPs for effective promoting photocatalytic activity and antibacterial activity through ROS generation during photoexcitation [39]. To date, even though many problems regarding PDT have been solved, issue like significant enhancement of ROS generation still needs further optimization.

In this article, we proposed a novel strategy of combining ZnO nanorods (NRs) with Au NPs to enhance ROS generation under UV irradiation. A facile solution method was utilized to decorate Au NPs on ZnO NRs with tunable molar ratio of ZnO:Au. Unlike most of previous reports, in which nanostructures usually worked as carriers for PSs or light transducers [3, 35, 36, 40-42], the so-synthesized nanohybrid was also responsible for the role of PS to induce ROS release. By introducing the semiconductor/metal heterostructure between ZnO and Au, the electron transfer at the interface was modulated when excited by UV, resulting in a considerable enhancement of ROS generation compared with pristine ZnO NRs or pristine Au NPs. Moreover, the samples with molar ratio (ZnO:Au) of 20:1 yielded the highest ROS generation because of the largest interface area, which in turn led to the lowest cell viability for Hela and C2C12 Cells after PDT treatment. In this case, the therapeutic efficacy on Hela cells was demonstrated to be remarkably improved due to the enhanced ROS generation by Au@ZnO nanohybrids.

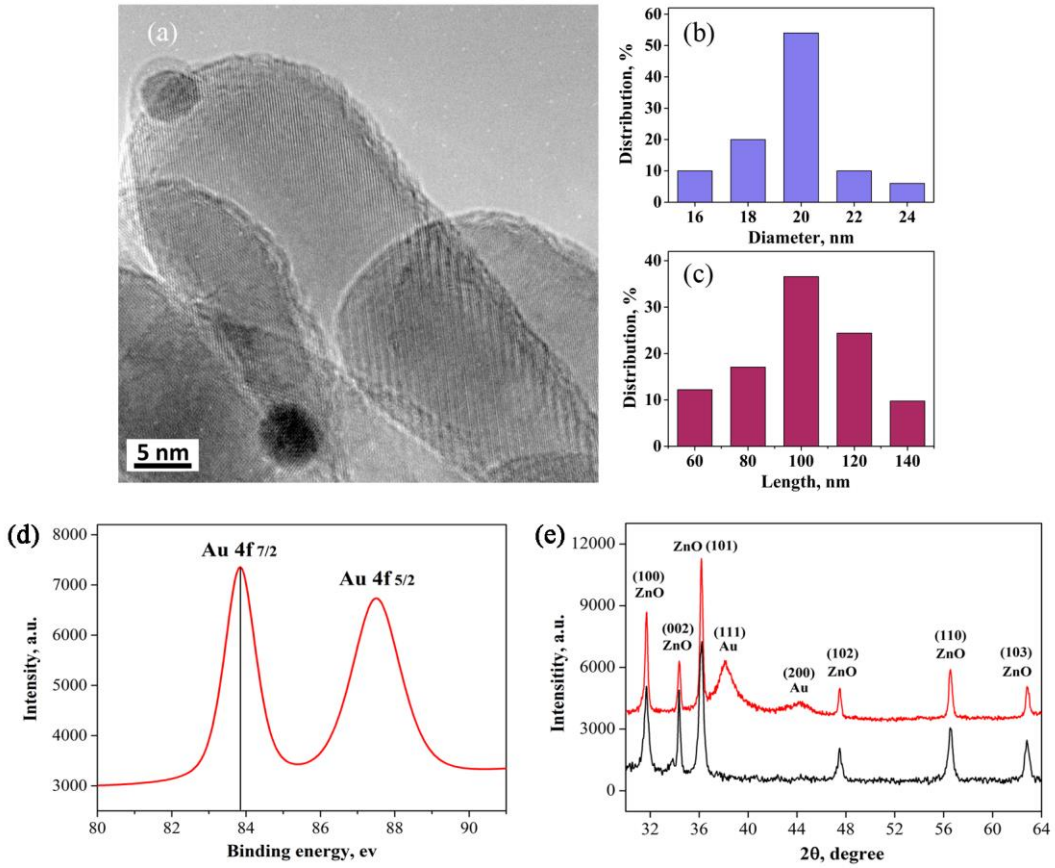

Figure 1 (a) HRTEM image of Au@ZnO (ZnO:Au=100:1) hybrid nanocrystals; (b) Diameter; (c) Length distribution of ZnO NRs; (d) Au 4f XPS spectra of Au@ ZnO, (e) XRD patterns of pristine ZnO NRs sample and Au@ZnO nanohybrids (ZnO:Au=100:1).

2 Results and discussion

Fig. 1a shows a typical TEM image of as-synthesized Au@ZnO nanohybrids, in which the high contrast difference between ZnO and Au is distinguishable because of the higher electron density of metal Au. The mean size of the nanorods is about 20nm in diameter (Fig. 1b) and 100nm in length (Fig. 1c), and the average diameter of the Au nanoparticles is about 5 nm. Since there are many single ionized oxygen vacancies (Vo^{+}) on the surface of ZnO nanorods, the surface energy of "active center" is higher than that of the nonpolar planes and is energetically favored to Au deposition [43]. It has been demonstrated that Au nanoparticles were not absorbed onto the ZnO nanorods physically, but nucleated and grew on the ZnO nanorods [44]. By adjusting the molar ratio of ZnO to $HAuCl_4$, varying amounts of Au NPs in the samples were acquired (Table 1). Specifically, for the nanohybrid with the molar ratio (ZnO:Au) of 100:1, it was calculated that there should be approximately 3.5 Au NPs per single ZnO NR.

Table 1 Characteristics of samples with various ZnO:Au molar ratio

Au NPs@ZnO NRs	100:1	50:1	20:1
ZnO NRs (mg/ml)	0.648	0.324	0.130
$HAuCl_4$ (μmol)	4	4	4
Au NPs/ single ZnO NRs	3.5	7	17.5

In order to characterize the chemical valence state of Au in NPs, XPS was performed (Fig. 1d). The spectra were calibrated with respect to the C1s line of

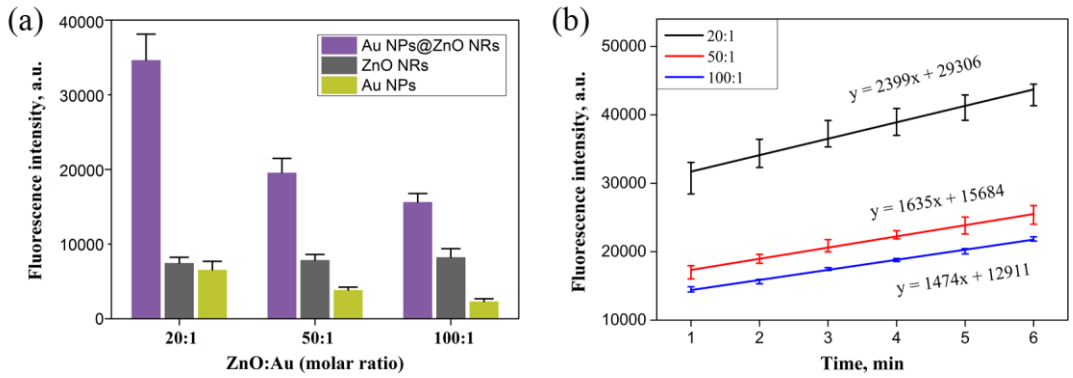

Figure 2 (a) Elevated ROS generation of nanohybrids with various ZnO:Au molar ratio (100 μg/ml was fixed) compared to pristine Au NPs and pristine ZnO NRs with corresponding concentrations after 2 min UV irradiation; (b) Kinetics of ROS generation induced by nanohybrids (100 μg/ml, ZnO:Au = 20:1, 50:1, 100:1) with UV irradiation for different durations (mean ± SD, n = 3). ROS was measured through fluorescence intensity with tracking agent DHR123.

adventitious carbon at 284.8 ev. The Au 4f $_{7/2}$ peak is centered at binding energy of 83.8 eV, with a slight shift of ~0.2 eV from the binding energy of bulk metallic gold (84.0 eV) [45]. This shift toward lower value can be attributed to the small size and negative charging of Au NPs. Hence, the deposited Au NPs are confirmed to be metallic elementary substance. The obtained X-ray diffraction patterns are in good agreement with the standard hexagonal wurtzite structure of ZnO (JCPDS 75-0576) and the diffraction peaks of (111) and (002) planes of the face-center cubic (fcc) gold (Fig. 1e). In addition, no other impurity phase and no remarkable shift of all diffraction peaks were detected.

In an aim to confirm the enhanced ROS generation induced by Au@ZnO nanohybrids, quantitative measurement of ROS formation should be carried out. However, the direct quantification of ROS yield is extremely challenging due to the short lifetime of ROS, so various ROS probes were developed for indirect measurement [46]. Here, nonfluorescent dihydrohodamine 123 (DHR123) was adopted as ROS tracking agent, which was oxidized to fluorescent Rhodamine 123 (R123) in the presence of ROS [47]. It is known that neither Au NPs nor ZnO NRs is fluorescent at the wavelength of 535 nm. Even though the surface-enhanced effect of Au NPs might have a little influence on fluorescence measurement, it could hardly cause any impact on the overall trend of the results due to the extremely low concentration of Au NPs in the complex solution [23]. Under this circumstance, the measured fluorescence intensity at 535 nm was basically proportional to the conversion of R123 from DHR123, that is, to the generated ROS concentration. As shown in Fig. 2a, enhanced ROS generation was confirmed through the fluorescence intensity detection. Clearly, for the Au@ZnO nanohybrids, the ROS yield was notably improved along with the variation of ZnO:Au molar ratio from 100:1 to 20:1 at a fixed concentration of 100 μg/ml. To better elucidate the enhancement effect, pristine Au NPs and pristine ZnO NRs with corresponding concentrations as that in the nanohybrids were introduced as comparisons. We found the ROS yields of the hybrids are much higher than that of the pristine ZnO NRs or the pristine Au NPs, and even higher than that of the sum of both, demonstrating the "1 + 1 > 2 effect" for the ROS generation enhancement. This phenomenon was demonstrated to be most significant in the 20:1 nanohybrids and a positive correlation between enhancement degree and the proportion of Au in the hybrid was confirmed. This indicated that such enhancement could be manipulated by the Au/ZnO interface area which was decided by the molar ratio of ZnO:Au in the nanohybrid. On the basis of fluorescence

intensity measurement, the time-resolved alteration of ROS yield in the presence of Au@ZnO nanohybrids (100 μg/ml) was also recorded in Fig. 2b. The ROS yield increased approximately linearly as the increase of the irradiation time. The 20:1 group obtained the highest slope, suggesting the fastest increase rate of the nanohybrid with the largest heterostructure interface area. Aside from these, the ROS yield against various nanohybrid concentrations ranging from 6.25 to 100 μg/ml was depicted in Fig. 3, suggesting an obvious dose-effect.

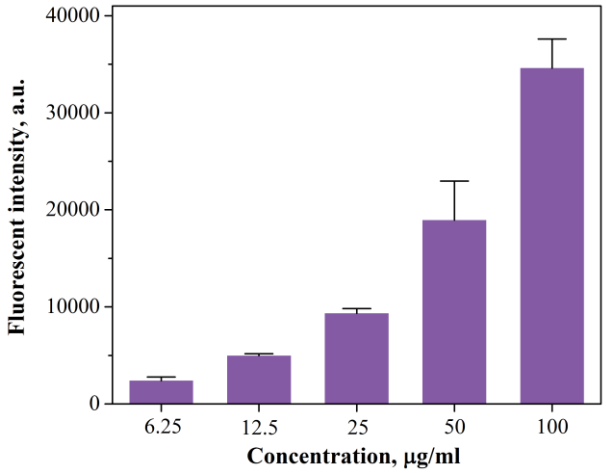

Figure 3 ROS yield after 2 min UV irradiation against various Au@ZnO nanohybrid concentration (mean ± SD, n = 3). The molar ratio of ZnO:Au was kept at 20:1.

To understand the phenomenon of enhanced ROS yield, the mechanism of ROS generation induced by photodynamic Au@ZnO nanohybrid is schematically displayed in Fig. 4. ZnO, with direct band gap of 3.36 eV, produce electron/hole pairs after exposure to UV irradiation. The photon-generated electrons in the conduction band and holes in the valence band would continuously induce a serious of photochemical reactions to generate ROS at ZnO NR surface in the aqueous solution [15]. Generally, electrons reduce O_2 to produce superoxide anion (O_2^-) while holes extract electrons from water and hydroxyl ions to produce hydroxyl radicals (·OH). On the other hand, at the surface of pristine Au NPs, UV irradiation results in producing photoelectrons and Augar electrons, which subsequently participate into the ROS generating reactions [22]. However, ZnO NRs and Au NPs do not only separately play their own roles contributing to the ROS generation during photochemical reactions, and the simple stacking of each effect from Au and ZnO is not sufficient to explain such great enhancement of ROS yield. Therefore, a possible explanation regarding interfacial coupling between metal Au and semiconductor ZnO in the heterostructure is proposed (Fig. 5). Since the work function of gold (5.1 eV) is lower than that of ZnO (5.2-5.3 eV) [48-50], the Fermi level of gold is higher than that of ZnO. Consequently, electrons transfer from Au to ZnO in order to equilibrate the Fermi energy level during the formation of Au@ZnO nanohybrids. The transferred electrons subsequently accumulate at the interface between ZnO and Au, causing a downward band bending at ZnO side. When UV irradiation is applied, electrons in ZnO are activated from valence band to conduction band. Due to the downward bend bending at the interface, the excited electrons are more inclined to flow to the Au side. For Au NPs, UV irradiation inspires photoelectrons and Augar electrons to take part in ROS generation. At meanwhile, the visible-light photons released by electron transition process from the defect energy levels in ZnO result in the surface plasmon resonance (SPR) at Au surface. The majority of excited electrons further contribute to generate ROS, while the minority excited electrons are injected back

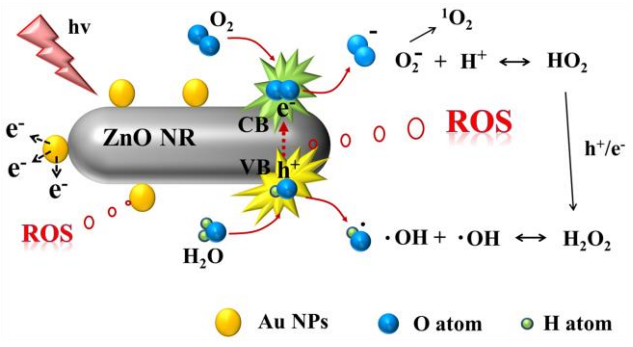

Figure 4 Schematic illustration of the proposed model for enhanced ROS generation induced by Au NPs@ZnO NRs hybrid under UV irradiation.

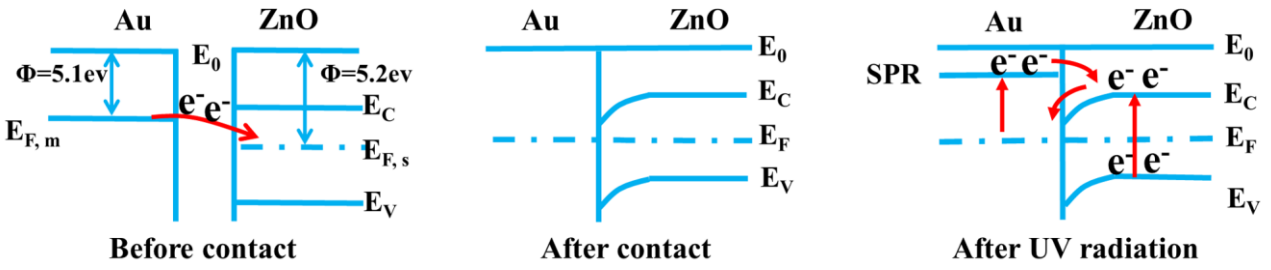

Figure 5 The energy level diagram of ZnO NRs and Au NPs before contact, after contact and under UV radiation.

to the conduction band of ZnO. A portion of the minority electrons jump back to the valence band for recombination and the rest of them further flow into Au along the downward bending band. In general, the band bending near the interface at ZnO side significantly facilitates electron transfer to Au side, thus considerably suppressing the electron-hole recombination amount in ZnO, and simultaneously increasing the amount of excited electrons with high energy at Au surface, which finally improves the efficiency of ROS generation.

To sum up, ZnO NRs and Au NPs contribute synergistically to form metal/semiconductor heterostructure to modulate electron transfer at interface, which in turn lead to the great enhancement of ROS generation. Here, the heterostructure interface is the key point. So it is reasonable to explain that the enhancement effect could be controlled by tuning the heterostructure interface area, that is, tuning the molar ratio of ZnO:Au in the hybrid. Consequently, it is acceptable for the 1 + 1 > 2 effect on the enhancement of ROS generation.

Prior to the application in PDT, we studied the cytotoxicity of so-synthesized nanohybrids toward Hela and C2C12 cell lines through thiazolyl blue tetrazolium bromide (MTT) assays. The results based on two cell lines in Fig. 6 are consistent, indicating that Au@ZnO nanohybrids were almost nontoxic even at a relatively high concentration of 100 μg/ml with the variation of ZnO:Au molar ratio from 100:1 to 20:1. However, the negligible impact on cell viability still existed, which could be attributed to the cytotoxicity mainly coming from ZnO NRs [15, 44].

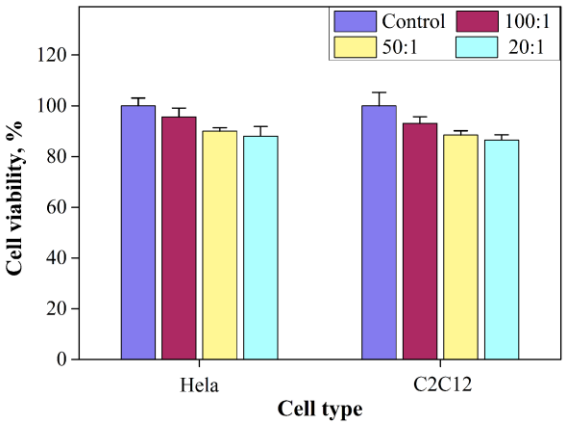

Figure 6 Toxicity test of Au@ZnO nanohybrids (100 μg/ml) based on Hela cells and C2C12 cells (mean ± SD, n = 3).

It has been reported that the light with a specific wavelength would excite the photosensitizing agent to generate ROS, which is believed to be responsible for selective tumor cell destruction [7]. And the therapeutic effect in PDT treatment closely correlated with the intracellular ROS level [23, 51]. Moreover, the cellular uptake of nanomaterials, such as gold, ZnO or even the composite in the size the same as so-synthesized nanohybrids have been widely demonstrated [15, 44, 52, 53]. As for Au@ZnO nanohybrids, the PDT efficacy against different molar ratio of ZnO:Au and different hybrid concentration on Hela (Fig. 7) and C2C12 cells (Fig.

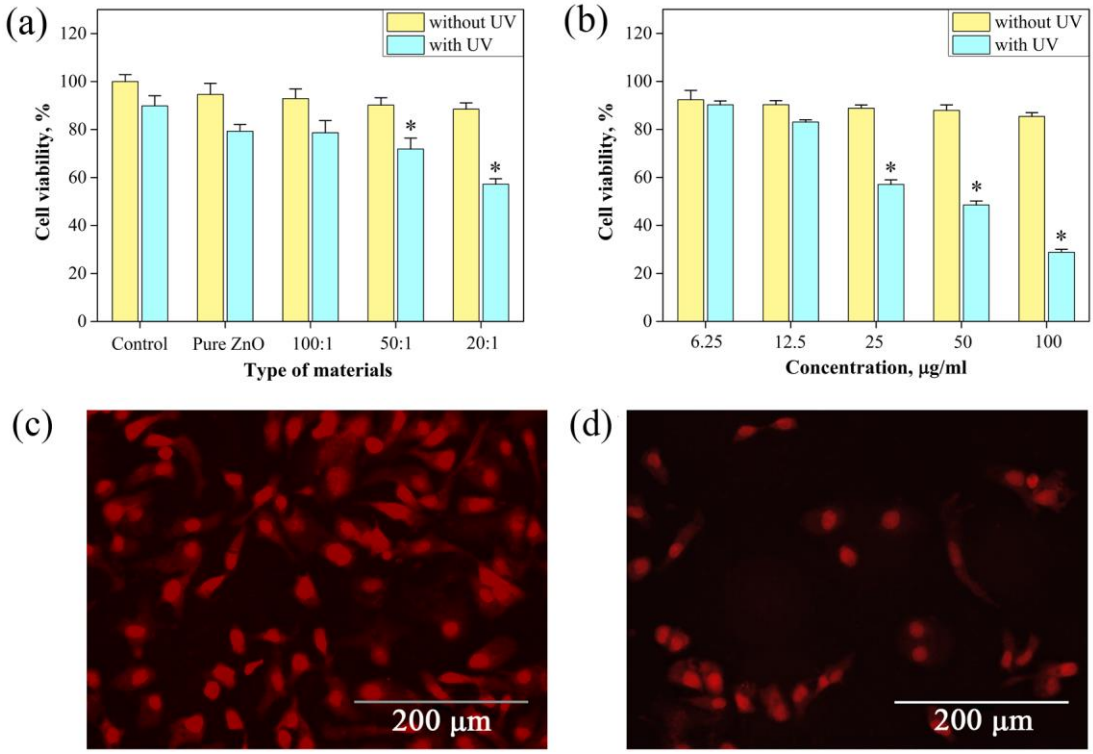

Figure 7 PDT experiment results based on Hela cells against (a) variation of ZnO:Au molar ratio (25 μg/ml was fixed) and (b) variation of nanohybrid concentration (ZnO:Au molar ratio of 20:1 was fixed) after 2 min UV irradiation (mean ± SD, n = 3). Typical fluorescence image of Hela cells before (c) and after (d) treatment of ZnO/Au nanohybrids (100 μg/ml, ZnO:Au = 20:1) under UV irradiation for 2 min. Scale bar dimensions are provided for each image.

S1) have been investigated. With the exposure to UV, 79% cell viability was acquired in the pristine ZnO group and around 56% cell viability was obtained for the 20:1 nanohybrids (25 μg/ml) (Fig. 7a). Noticeably, with the increase of the proportion of Au in nanohybrids, the PDT efficacy on Hela cells was obviously strengthened, and the cell destruction ratio was 2.01:1.31:1 with various ZnO:Au molar ratio of 20:1, 50:1 and 100:1. The result is basically consistent with ROS generation enhancement ratio of 2.22:1.25:1 characterized by ROS tracking agent (Fig. 3a). However, even though the hybrid of 100:1 yielded much more ROS than pristine ZnO, they did not perform significant difference in the cell viability. The reason might be the elaborate ROS defense mechanism of cells at a relatively low ROS concentration, so there is a threshold value of ROS concentration for cell damage. Moreover, the dose dependence of PDT efficacy was confirmed with the variation of nanohybrid concentration at a fixed molar ratio of 20:1 (Fig. 7b). The trend of cell destruction against nanohybrid concentration is also in agreement with the quantitative analysis of ROS generation in Fig 4. It is worth pointing out that the nanohybrid of 100 μg/ml yielded the Hela cell viability as low as 28% after the exposure to UV for 2 min. In Fig. 7c and 7d, it can be seen that the number of living Hela cells dramatically decreased and the cell shape obviously changed, suggesting the remarkable PDT efficacy of Au@ZnO nanohybrids. This is coherent with the MTT assay results of PDT experiments.

3 Conlusions

To summarize, we have explored the feasibility of

combining ZnO NRs and Au NPs for enhanced ROS generation and PDT. The introduction of Au/ZnO metal/semiconductor heterostructure considerably enhanced ROS generation under UV irradiation, and then a possible explanation regarding the modulation of electron transfer at the interface was proposed. Moreover, such enhancement was strengthened along with the increase of Au/ZnO interface area, that is, the proportion of Au in the hybrid. We have also shown that the cell viabilities of Hela and C2C12 cells were significantly influenced during the PDT in the presence of so-synthesized nanohybrid under UV irradiation, confirming the potential of adopting Au@ZnO hybrids in PDT application for comprehensive cancer treatment.

4 Methods

Gold (III) chloride trihydrate ($HAuCl_4.3H_2O$), dihydrohodamine-123 (DHR123) were purchased from sigma-Aldrich (St.Louis, MO, USA). $Zn(Ac)_2.2H_2O$, NaOH, ethanol, trisodiuom citrate and polyethylene glycol 400 (PEG-400) were purchased from Beijing Chemical Works. They were used without further purification.

For Synthesis of Au NPs@ZnO NRs Hybrid, 4 mmol Zn(Ac)2.2H2O and 32 mmol NaOH were separately dissolved into 90 ml and 50 ml absolute ethanol, after mixing them together under magnetic stirring, 32 ml PEG-400 was introduced into above solution. Then the reaction was kept at 140 °C for 16 h in a Teflon-lined stainless autoclave tank. The obtained precipitations were washed by absolute ethanol and deionized water for several times, and then dried in vacuum at 60 °C. Au NPs@ZnO NRs hybrid nanocrystals with varying amounts of Au nanoparticles have been synthesized by adjusting the molar ratio of ZnO to $HAuCl_4$ through a general and simple aqueous-based method [44, 50]. Taking 100:1 molar ratio of ZnO:Au for example, as-prepared ZnO were suspended in 50ml diluted trisodiuom citrate solution (0.648 mg/ml) by ultrasonic treatment, and then was precipitated by dropwise adding 2 ml dilute $HAuCl_4$ (0.002 mol/L). The mixed solution was stirred at room temperature for about 12 h, followed by a gradually color-change from pale yellow to lilac. These nanohybrid products were collected by centrifugation and washed with distilled water and ethanol several times for further characterization.

The morphology and size distribution of the product were determined by transmission electron microscopy (TEM, JEOL, JEM-100CX II, Japan). The high-resolution TEM images were acquired using acceleration voltage of 300 kV. TEM samples were prepared by placing a drop of diluted suspended product solution onto a carbon-coated copper grid and allowing it to dry in air. The crystal structure and phase identification of the nanohybrid was determined by X-ray diffraction patterns recorded on an X-ray diffractometer (Rigaku DMAX-RB, Japan, CuKα). Chemical states of surface element of Au NPs were investigated by X-ray photoelectron spectroscopy (XPS, Kratos AXIS ULTRA DLD, SHIMADZU, Japan), using Al Kα as an exciting X-ray source.

To explore the kinetics of ROS formation, Au NPs@ZnO NRs hybrid solutions (50 μL) of various concentrations and various ZnO:Au molar ratio, pristine Au NPs (50 μL) or pristine ZnO NRs (50 μL) with corresponding concentrations were mixed with 50 μL of 10 μM DHR123 under dark condition. Here, DHR123 (nonfluorescent) was oxidized by ROS to form fluorescent Rhodamine 123 (R123), thus working as ROS tracking agent. Total volume of 100 μL samples (n = 3) in 96-well plates were irradiated by UV irradiation (λ = 254 nm, 0.1 mW/cm^2) for different time durations. The fluorescence measurements were done after each 1 min irradiation using a multilabel plate reader (VICTOR™ X2, PerkinElmer, USA) at an excitation wave length of 485 nm and an emission wavelength of 535 nm.

For cell culture, human uterine carcinoma cell line (HeLa) and mouse myoblast cell line (C2C12) were purchased from ATCC (Manassas, VA). The Dulbecco's Modified Eagle Medium-high glucose (HyClone, MA), added 10% fetal bovine serum (HyClone, MA) and Penicillin/Streptomycin (100 U/mL and 100 μg/mL, respectively, PAA Laboratories GmbH, Austria) was used as the culture medium. Remove cell from liquid nitrogen and immediately

place in 37 °C water bath and quickly shake until thawed. Quickly pipette cell into a 25 cm^2 flask, add 5 mL medium and place back in incubator (37 °C, 5% CO_2). Change culture media to remove non-adherent cells after 16-24 h. Cells were seeded into a 96-well plate at a density of 2×10^4 cells per well and then cultured for 48 h prior to the further treatment.

To determine the cell cytotoxicity, cells in 96-well plates, were exposed to pristine ZnO nanorods and nanohybrid solution at varying ZnO:Au molar ratio (100:1, 50:1, 20:1). After 24 h inubation at 37 °C and 5% CO_2, the tetrazolium salt 3-(4,5-dimethylthiazol -2-yl)-2.5-diphenyltetrazoliumbromide (MTT, sigma) was added into each well. After another 4 h, nonreacted solution was removed and dimethyl sulf-oxide (DMSO, sigma) was added to extract the formazan crystals followed by the 15 min shaking. Then the optical absorbance of the extract was measured at 490 nm (Sunrise, TECAN, Switzerland). Controls were cultivated under the same conditions without addition of any nanohybrid product. The experiment was repeated at least three times. Cell viability was expressed as follows: cell viability (%) = [A]test/[A]control*100%, where [A]test and [A]control represent the optical density at 490 nm for the test and control experiments, respectively.

For PDT experiments, the procedure of cell culture and treatment of nanohybrid was similar with the above mentioned. After incubation for 12 h with the medium containing nanohybrid products, UV irradiation (2.4 $\mu W/cm^2$) was on the top of the cells for 2 min. Then the cells were incubated for another 12 h prior to cell viability assessment through MTT assay.

Acknowledgements

This work was supported by the National Major Research Program of China (2013CB932600), the Major Project of International Cooperation and Exchanges (2012DFA50990), the Program of Introducing Talents of Discipline to Universities, the National Natural Science Foundation of China (51232001, 51172022, 51372023, 31371203), the Research Fund of Co-construction Program from Beijing Municipal Commission of Education, the Fundamental Research Funds for the Central Universities, the Program for Changjiang Scholars and Innovative Research Team in University.

References

[1] Guo, H.; Qian, H.; Idris, N. M.; Zhang, Y. Singlet oxygen-induced apoptosis of cancer cells using upconversion fluorescent nanoparticles as a carrier of photosensitizer. *Nanomedicine* **2010**, 6, 486-495.

[2] Bae, B.-c.; Na, K. Self-Quenching Polysaccharide -based nanogels of pullulan/folate-photosensitizer conjugates for photodynamic therapy. *Biomaterials* **2010**, 31, 6325-6335.

[3] Idris, N. M.; Gnanasammandhan, M. K.; Zhang, J.; Ho, P. C.; Mahendran, R.; Zhang, Y. In vivo photodynamic therapy using upconversion nanoparticles as remote-controlled nanotransducers. *Nat. Med.* **2012**, 18, 1580-1585.

[4] Kato, H. Photodynamic therapy for lung cancer - a review of 19 years' experience, *J. Photochem. Photobiol.* **1998**, B 42, 96-99.

[5] Schuller, D.E.; McCaughan Jr., J.S.; Rock, R.P. Photodynamic therapy in head and neck cancer, *Arch. Otolaryngol.* **1985**, 111, 351-355.

[6] Skyrme, R.J.; French, A.J.; Datta, S.N.; Allman, R.; Mason, M.D.; Matthews, P.N.; A phase-1 study of sequential mitomycin C and 5-aminolaevulinic acid-mediated photodynamic therapy in recurrent superficial bladder carcinoma, *BJU Int.* **2005**, 95, 1206-1210.

[7] Rhodes, L.E.; de Rie, M.; Enstrom, Y.; Groves, R.; Morken, T.; Goulden, V.; Wong, G.A.; Grob, J.J.; Varma, S.; Wolf, P.; Photodynamic therapy using topical methyl aminolevulinate vs surgery for nodular basal cell carcinoma: results of a multicenter randomized prospective trial, *Arch. Dermatol*. **2004**, 140, 17-23.

[8] Henderson, B. W.; Dougherty, T. J. How does photodynamic therapy work? *Photochem. Photobiol.* **1992**, 55, 145-157.

[9] He, X.; Wu, X.; Wang, K.; Shi, B.; Hai, L. Methylene blue-encapsulated phosphonate- terminated silica nanoparticles for simultaneous in vivo imaging and photodynamic therapy. *Biomaterials* **2009**, 30, 5601-5609.

[10] Celli, J. P.; Spring, B. Q.; Rizvi, I.; Evans, C. L.; Samkoe, K. S.; Verma, S.; Pogue, B. W.; Hasan, T. Imaging and photodynamic therapy: mechanisms, monitoring, and optimization. *Chem. Rev.* **2010**, 110, 2795-2838.

[11] Dougherty, T. J.; Gomer, C. J.; Henderson, B. W.; Jori, G.; Kessel, D.; Korbelik, M.; Moan, J.; Peng, Q. Photodynamic therapy. *J. Nat. Cancer Inst.* **1998**, 90, 889-905.

[12] Foote, C. S. Photosensitized oxygenations and the role of singlet oxygen. *Acc. Chem. Res.* **1968**, 1, 104-110.

[13] Buttke, T. M.; Sandstrom, P. A. Oxidative stress as a mediator of apoptosis. *Immunol. Today* **1994**, 15, 7-10.

[14] Brown, S. B.; Brown, E. A.; Walker, I. The present and future role of photodynamic therapy in cancer treatment. *Lancet Oncol.* **2004**, 5, 497-508.

[15] Zhang, H.; Chen, B.; Jiang, H.; Wang, C.; Wang, H.; Wang, X. A strategy for zno nanorod mediated multi-mode cancer treatment. *Biomaterials* **2011**, 32, 1906-1914.

[16] Guo, D.; Wu, C.; Jiang, H.; Li, Q.; Wang, X.; Chen, B. Synergistic cytotoxic effect of different sized ZnO nanoparticles and daunorubicin against leukemia cancer cells under UV irradiation. *J.Photochem. Photobio.B* **2008**, 93, 119-126.

[17] Ostrovsky, S.; Kazimirsky, G.; Gedanken, A.; Brodie, C. Selective cytotoxic effect of zno nanoparticles on glioma cells. *Nano Res.* **2009**, 2, 882-890.

[18] Li, J.; Guo, D.; Wang, X.; Wang, H.; Jiang, H.; Chen, B. The photodynamic effect of different size ZnO nanoparticles on cancer cell proliferation in vitro. *Nanoscale Res. Lett.* **2010**, 5, 1063-1071.

[19] Zhang, Y.; Chen, W.; Wang, S.; Liu, Y.; Pope, C. Phototoxicity of Zinc Oxide nanoparticle conjugatesin human ovarian cancer NIH: OVCAR-3 Cells. *J. Biomed. Nanotechnol.* **2008**, 4, 432-438.

[20] Ahamed, M.; Akhtar, M. J.; Raja, M.; Ahmad, I.; Siddiqui, M. K. J.; AlSalhi, M. S.; Alrokayan, S. A. ZnO nanorod-induced apoptosis in human alveolar adenocarcinoma cells via P53, survivin and Bax/Bcl-2 Pathways: role of oxidative stress. *Nanomedicine* **2011**, 7, 904-913.

[21] Dutta, R.; Nenavathu, B. P.; Gangishetty, M. K.; Reddy, A. Studies on antibacterial activity of ZnO nanoparticles by ROS induced lipid peroxidation. *Colloids Surf. B* **2012**, 94, 143-150.

[22] Misawa, M.; Takahashi, J. Generation of reactive oxygen species induced by gold nanoparticles under X-ray and UV irradiations. *Nanomedicine* **2011**, 7, 604-614.

[23] Khaing Oo, M. K.; Yang, Y.; Hu, Y.; Gomez, M.; Du, H.; Wang, H. Gold nanoparticle-enhanced and size-dependent generation of reactive oxygen species from protoporphyrin IX. *ACS Nano* **2012**, 6, 1939-1947.

[24] Minai, L.; Yeheskely-Hayon, D.; Yelin, D. High levels of reactive oxygen species in gold nanoparticle-targeted cancer cells following femtosecond pulse irradiation. *Sci. Rep.* **2013**, 3. 2146.

[25] Wang, S.; Chen, K. J.; Wu, T. H.; Wang, H.; Lin, W. Y.; Ohashi, M.; Chiou, P. Y.; Tseng, H. R., Photothermal effects of supramolecularly assembled gold nanoparticles for the targeted treatment of cancer cells. *Angew. Chem. Int. Edit.* **2010**, 49, 3777-3781.

[26] Zhao, Y.; Jiang, X. Multiple strategies to activate gold nanoparticles as antibiotics. *Nanoscale* **2013**, 5, 8340-8350.

[27] Khaing Oo, M. K.; Yang, X.; Du, H.; Wang, H. 5-Aminolevulinic acid-conjugated gold nanoparticles for photodynamic therapy of cancer. *Nanomedicine (Lond)* **2008**, 3, 777-786.

[28] Wang, J.; Zhu, G.; You, M.; Song, E.; Shukoor, M. I.; Zhang, K.; Altman, M. B.; Chen, Y.; Zhu, Z.; Huang, C. Z. Assembly of aptamer switch probes and photosensitizer on gold nanorods for targeted photothermal and photodynamic cancer therapy. *ACS Nano* **2012**, 6, 5070-5077.

[29] Tong, L.; Zhao, Y.; Huff, T. B.; Hansen, M. N.; Wei, A.; Cheng, J. X. Gold nanorods mediate tumor cell death by compromising membrane integrity. *Adv. Mater*. **2007**, 19, 3136-3141.

[30] Li, J. L.; Day, D.; Gu, M. Ultra‐low energy threshold for cancer photothermal therapy using transferrin-conjugated gold nanorods. *Adv. Mater.* **2008**, 20, 3866-3871.

[31] Jang, B.; Park, J.-Y.; Tung, C.-H.; Kim, I.-H.; Choi, Y. Gold nanorod−photosensitizer complex for near-infrared fluorescence imaging and photodynamic/photothermal therapy in vivo. *ACS Nano* **2011**, 5, 1086-1094.

[32] Choi, W. I.; Kim, J.-Y.; Kang, C.; Byeon, C. C.; Kim, Y. H.; Tae, G. Tumor regression in vivo by photothermal therapy based on gold-nanorod-loaded, functional nanocarriers. *ACS Nano* **2011**, 5, 1995-2003.

[33] Wang, N.; Zhao, Z.; Lv, Y.; Fan, H.; Bai, H.; Meng, H.; Long, Y.; Fu, T.; Zhang, X.; Tan, W., Gold nanorod-photosensitizer conjugate with extracellular pH-driven tumor targeting ability for photothermal/photodynamic therapy. *Nano Res.* **2014**, 7, 1291-1301.

[34] Terentyuk, G.; Panfilova, E.; Khanadeev, V.; Chumakov, D.; Genina, E.; Bashkatov, A.; Tuchin, V.; Bucharskaya, A.; Maslyakova, G.; Khlebtsov, N. et al. Gold nanorods with a hematoporphyrin-loaded silica shell for dual-modality photodynamic and photothermal treatment of tumors in vivo. *Nano Res.* **2014**, 7, 325-337.

[35] Gao, L.; Fei, J.; Zhao, J.; Li, H.; Cui, Y.; Li, J. Hypocrellin-Loaded Gold Nanocages with High Two-Photon Efficiency for Photothermal/ Photodynamic Cancer Therapy in Vitro. *ACS NANO* **2012**, 6, 8030-8040.

[36] Xia, Y.; Li, W.; Cobley, C. M.; Chen, J.; Xia, X.; Zhang, Q.; Yang, M.; Cho, E. C.; Brown, P. K. Gold nanocages: from synthesis to theranostic applications. *Acc. of chem. Res.* **2011**, 44, 914-924.

[37] Liu, H.; Chen, D.; Tang, F.; Du, G.; Li, L.; Meng, X.; Liang, W.; Zhang, Y.; Teng, X.; Li, Y. Photothermal therapy of lewis lung carcinoma in mice using gold nanoshells on carboxylated polystyrene spheres. *Nanotechnology* **2008**, 19, 455101.

[38] Li, C.; Chen, T.; Ocsoy, I.; Zhu, G.; Yasun, E.; You, M.; Wu, C.; Zheng, J.; Song, E.; Huang, C. Z.; Tan, W., Gold-coated Fe3O4 nanoroses with five unique functions for cancer cell targeting, imaging, and therapy. *Adv. Func. Mater*. **2014**, 24, 1772-1780.

[39] He, W.; Kim, H.-K.; Wamer, W. G.; Melka, D.; Callahan, J. H.; Yin, J.-J., Photogenerated charge carriers and reactive oxygen species in ZnO/Au hybrid nanostructures with enhanced photocatalytic and antibacterial activity. *J. Am. Chem. Soc.* **2013**, 136, 750-757.

[40] Chatterjee, D. K.; Fong, L. S.; Zhang, Y. Nanoparticles in photodynamic therapy: an emerging paradigm. *Adv. Drug Deliv. Rev.* **2008**, 60, 1627-1637.

[41] Paszko, E.; Ehrhardt, C.; Senge, M. O.; Kelleher, D. P.; Reynolds, J. V. Nanodrug applications in photodynamic therapy. *Photodiagn. Photodyn.* **2011**, 8, 14-29.

[42] Shan, J.; Budijono, S. J.; Hu, G.; Yao, N.; Kang, Y.; Ju, Y.; Prud'homme, R. K. Pegylated composite nanoparticles containing upconverting phosphors and meso-tetraphenyl porphine (TPP) for photodynamic therapy. *Adv. Func. Mater.* **2011**, 21, 2488-2495.

[43] Diebold, U.; Koplitz, L. V.; Dulub, O. Atomic-scale properties of low-index ZnO surfaces. *Appl. Surf. Sci.* **2004**, 237, 336-342.

[44] Zhang, W.-Q.; Lu, Y.; Zhang, T.-K.; Xu, W.; Zhang, M.; Yu, S.-H. Controlled synthesis and biocompatibility of water-soluble ZnO nanorods/Au nanocomposites with tunable UV and visible emission intensity. *J. Phys. Chem. C* **2008**, 112, 19872-19877.

[45] Fu, Q.; Saltsburg, H.; Flytzani-Stephanopoulos, M. Active nonmetallic Au and Pt species on ceria-based water-gas shift catalysts. *Science* **2003**, 301, 935-938.

[46] Soh, N. Recent advances in fluorescent probes for the detection of reactive oxygen species. *Anal. Bioanal. Chem.* **2006**, 386, 532-543.

[47] Crow, J. P. Dichlorodihydrofluorescein and dihydrorhodamine 123 are sensitive indicators of peroxynitrite in vitro: implications for intracellular measurement of reactive nitrogen and oxygen species. *Nitric oxide* **1997**, 1, 145-157.

[48] Bai, X.; Wang, E. G.; Gao, P.; Wang, Z. L. Measuring the work function at a nanobelt tip and at a nanoparticle surface. *Nano Lett.* **2003**, 3, 1147-1150.

[49] Wang, X.; Summers, C. J.; Wang, Z. L., Self-attraction among aligned Au/ZnO nanorods under electron beam. *Appl. Phys. Lett.* **2004**, 86, 013111.

[50] Wang, X.; Kong, X.; Yu, Y.; Zhang, H. Synthesis and characterization of water-soluble and bifunctional ZnO-Au nanocomposites. *J. Phys. Chem. C* **2007**, 111, 3836-3841.

[51] Cui, S.; Yin, D.; Chen, Y.; Di, Y.; Chen, H.; Ma, Y.; Achilefu, S.; Gu, Y. In vivo targeted deep-tissue photodynamic therapy based on near-infrared light triggered upconversion nanoconstruct. *ACS NANO* **2012**, 7, 676-688.

[52] Zhao, F.; Zhao, Y.; Liu, Y.; Chang, X.; Chen, C.; Zhao, Y. Cellular uptake, intracellular trafficking, and cytotoxicity of nanomaterials. *Small* **2011**, 7, 1322-1337.

[53] Chithrani, B. D.; Ghazani, A. A.; Chan, W. C. Determining the size and shape dependence of gold nanoparticle uptake into mammalian cells. *Nano Lett.* **2006**, 6, 662-668.